SYNTHESIS AND CHARACTERIZATION OF POLYMER CERAMIC COMPOSITES

Thesis Submitted for the Award of the Degree of

Master of Science

By

SMRUTIREKHA SWAIN

Under the Academic Autonomy

National Institute of Technology, Rourkela

Under the Guidance of

Dr. Dillip Kumar Pradhan

Department of Physics

National Institute of Technology

Rourkela-769008

Department of Physics

National Institute of Technology

Rourkela – 769008 (Orissa)

Certificate

This is to certify that the thesis entitled "**Synthesis and Characterization of Polymer Ceramic Composites**" being submitted by **Smrutirekha Swain** in partial fulfillment of the requirements for the award of the degree of Master of Science in Physics at National Institute of Technology, Rourkela is an authentic work carried out by her under my supervision. To the best of my knowledge, the matter embodied in the thesis has not been submitted to any other University/Institute for the award of any degree or diploma.

Date

Dillip Kumar Pradhan

ACKNOWLEDGEMENT

I humbly prostrate myself before the Almighty for his grace and abundant blessings which enabled me to complete this work successfully.

It gives me immense pleasure to express my deep sense of gratitude to my supervisor **Prof. Dillip Kumar Pradhan** for his invaluable guidance, motivation constant inspiration and above all his ever co-operating attitude enabled me in bringing up this thesis in present elegant form.

I am extremely thankful to Prof. Biplab Ganguly, Head, Department of Physics and the faculty members of Physics department for providing all kinds of possible help and advice during the course of this work.

I am extremely thankful to Mr. Barun Kumar Barick and Mr. Satya Narayan Tripathy, Research Scholar, Department of Physics, for their valuable suggestions and constant help for this work. I am greatly thankful to all the research scholars of the department and my class mates for their inspiration and help.

I record my sincere thanks to Department of Ceramic Engineering, for the help in taking XRD, Department of Metallurgical and Material Science for extending all facilities to carry out the SEM, and Department of Chemistry for taking the FTIR spectrum.

I cherish to acknowledge the benevolence of my parents, brother and friends for their constant love, encouragement, enthusiasm, blessing, co-operation and support during the entire course of study.

Lastly I sincerely thank to all those who have directly or indirectly helped for the work reported here in.

Smrutirekha Swain

DEDICATED TO MY

PARENTS

ABSTRACT

The polycrystalline samples of $(Na_{0.5}\ Bi_{0.5})_{1-x}Nd_xTi_{(1-x/4)}O_3$ with x=0, 0.02, 0.04, 0.06 were prepared by high temperature solid state reaction technique. The formations of the compounds were confirmed by X-Ray diffraction (XRD) analysis. A systematic change in crystal structure from rhombohedral to tetragonal to cubic on Nd substitution was observed. The crystallite size and strain in the samples were calculated using Williamson Hall method**.** Fourier transform infrared spectroscopy (FTIR) analysis confirms the formation of perovskite structure. The polymer ceramic composites were prepared using polyvinylidene fluoride (PVDF) as polymer matrix and $Na_{0.5}Bi_{0.5}TiO_3$ (NBT) as ceramics powder by cold pressing technique. The microstructure/surface morphology of the ceramic oxide samples and composite was analyzed by scanning electron microscope.

CONTENTS

CHAPTER-1

INTRODUCTION

In recent years material scientists around the globe are involved in research and development of new multifunctional ceramic materials for many device applications such as multilayer capacitors, optical shutters and modulators, computer memory and display, microwave communication devices, piezoelectric detectors, ferroelectric random access memory (FRAM) etc [1-3]. In view of the device applications, Ferroelectric materials have occupied a significant position in the field of material research because of their huge applications in various electronic, optoelectronic, computer memory and communication devices [1, 3].

Ferroelectric materials can be studied in the form of single crystal or in the form of polycrystalline ceramic oxides. For the study of ferroelectric properties, homogeneous single crystal is usually preferred due to minimum effect of surfaces and imperfections. But single crystals require particular care in their preparation, cutting and polishing to make them suitable for device applications. So ceramics can be considered as substitutes for single crystals because of the following reasons; (i) it is easier to fabricate/synthesize ceramics into different shapes and sizes than their single crystal counterparts. (ii) there are additional structural/microstuctural feature (i.e. grain shape, size and porosity, etc). These microstructural features can be exploited in the design of the electro-ceramic materials for particular device requirements. The presence of grain boundaries gives rise to additional effect and play an important role for various physical properties, which is not present in single crystals. (iii) Ceramics oxides also posses good thermal, chemical and mechanical stability [1, 3].

Barium titanate ($BaTiO_3$) is the first ferroelectric ceramic belongs to perovskite structure discovered in 1945 and is used in capacitor application and piezoelectric transducer devices applications [1]. After the discovery of ferroelectricity in $BaTiO_3$, a large number of ferroelectric

oxides of different structural family have been discovered and studied to find out their suitability for various device applications. After the widespread use of $BaTiO_3$ many other ferroelectric ceramics including lead titanate ($PbTiO_3$), lead zirconate titanate (PZT), lead lanthanum zirconate titanate (PLZT), and relaxor ferroelectrics like lead magnesium niobate (PMN) have been developed and utilized for a variety of applications.

One of the most extensively studied groups of ceramic materials belongs to the ferroelectric compounds, which is a subgroup of dielectrics. A dielectric is an electrical insulator that can be polarized by the action of an applied electric field [4]. Dielectrics are broadly divided into two classes.

1. Polar dielectrics
2. Non-polar dielectrics

A dielectric having finite and permanent polarization even in the absence of electric field is known as polar dielectrics and the dielectrics where there is no such permanent polarization is called non-polar dielectrics. In the present study we will consider the case of polar class of materials.

1.1. Ferroelectrics and Related Materials

There are large numbers of crystals exising in nature. Based on the crystal symmetry they all can be grouped together into 230 space groups. Again these 230 space groups can be further divided into 32 point groups. Out of these 32 point groups 11 are centrosymmetric (i.e., the centre of the positive charge coincides with the centre of the negative charge) and 21 are noncentrosymmetric (i.e. the centre of the positive charge and the center of the negative charge does not coincide). Out of 21 non centrosymmetric point group, except one point group all are

piezoelectric. 10 out of the 20 point groups are called pyroelectric. They are also called polar crystals as they show the property of spontaneous polarization i.e. they exhibit electric dipole moment even in the absence of external electric field. Ferroelectric is a sub group of pyroelectric which is also a subgroup of piezoelectric. An inter relationship of piezoelectric and subgroups on the basis of symmetry is given in Fig. 1.

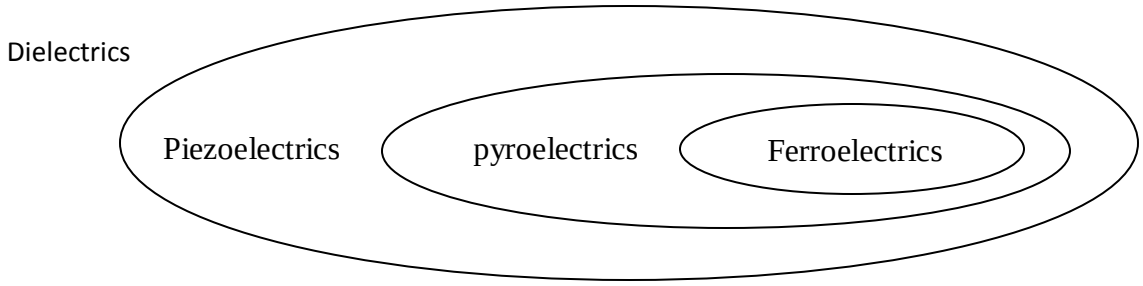

Fig. 1. Venn diagram showing the relationship between ferroelectrics, pyroelectrics and piezoelectrics

Crystals are said to be ferroelectric if the magnitude and direction of spontaneous polarization can be reversed by application of an external electric field. The reversal of spontaneous polarization was first observed in Rochelle salt by Valasek in 1920 [5]. The value of the spontaneous polarization depends upon the temperature. The variation of the spontaneous polarization with temperature for a ferroelectric crystal is shown in Fig-2. From the figure it is observed that the spontaneous polarization decreases with increase in temperature. At certain temperature the polarization disappears discontinuously or sometimes continuously, this is known as Curie point (T_c). The crystal does not exhibit ferroelectricity above the curie temperature and temperature below Curie point it is ferroelectric. At T_c there is a transition from ferroelectric state to paraelectric state. The room temperature dielectric constant of most of the ferroelectric materials are high and is maximum at T_c. Above T_c, the temperature dependent of

the dielectric constant obeys Curie Weiss law. $\varepsilon = \varepsilon_0 + \frac{C}{T - T_c}$, where ε is the permittivity of the material, ε_0 is the permittivity in vacuum, C is the Curie constant, T is the working temperature, T_c is the paraelectric Curie point or temperature at which the spontaneous polarization is zero.

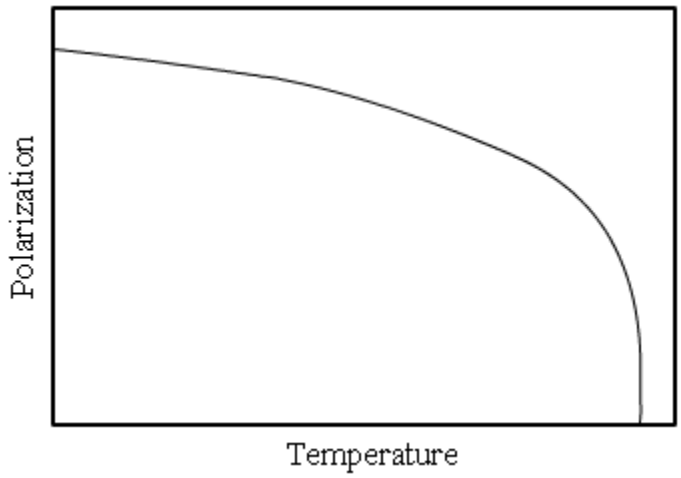

Fig. 2. Temperature dependence of the spontaneous polarization

In Ferroelectric crystals there are regions with uniform polarization called ferroelectric domains where all the electric dipoles are aligned in the same direction. The most important characteristics of ferroelectric materials is the non linear relationship between the polarization and the field giving rise to a hysteresis as shown in Fig-3. An increase in the electric field strength gives rise to a rapid increase in the polarization and above certain applied field, the polarization saturate known as saturate polarization (P_s). When the external field is removed some of the domains remain aligned in the positive direction and the polarization doesn't fall to zero even if the applied field is zero. This is known as Remnant Polarization (P_r). The external field needed to reduce the polarization to zero is called coercive field strength (E_c).

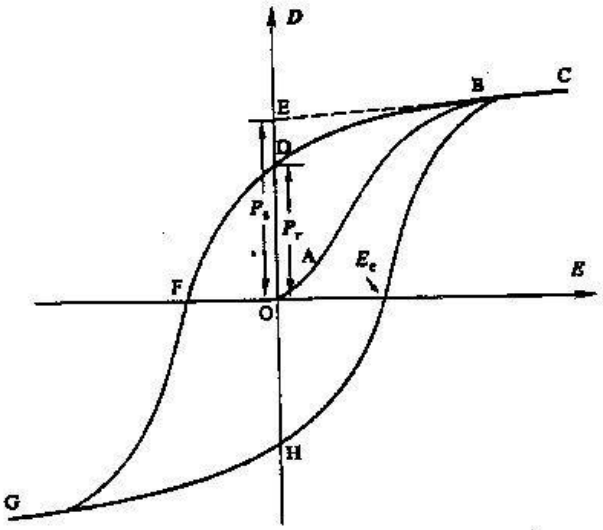

Fig. 3. Non linear relationship between the polarization and the electric field

1.2. Phase Transition

When the crystal structure changes with temperature in dielectric materials, then the materials undergo a phase transition. All the phase transitions in the crystals are due to change in the forces of interaction between the atoms in the crystals. The phase change results in various new properties of the crystals. The phase transition that changes the spontaneous polarization is called ferroelectric phase transitions. Phase transition can be classified into (i) First order phase transition (ii) Second order phase transition. In case of first order phase transition, the order parameter (in case of ferroelectric the order parameter is polarization) change discontinuously at transition point. If these parameters change continuously then the transition is called second order [4].

The most important group of ferroelectric ceramic is the family of oxygen octahedral which can be further classified into four types. They are

(1) Perovskite type
(2) Tungsten-Bronze type

(3) Spinel structure (Layered structure)

(4) Pyrochloro type

Among them perovskite ferroelectric ceramics oxides is the most studied one because of their wide variety of technological applications. The perovksite structure needs some explanation as the material under investigation belongs to this group. The simple perovskite structure has a general formula ABO_3, where A is a large mono or divalent cation, B is a small tetra to pentavalent cation. It is cubic with A atoms at the cubic corner, B atoms at the body center and oxygen atoms at the face center.

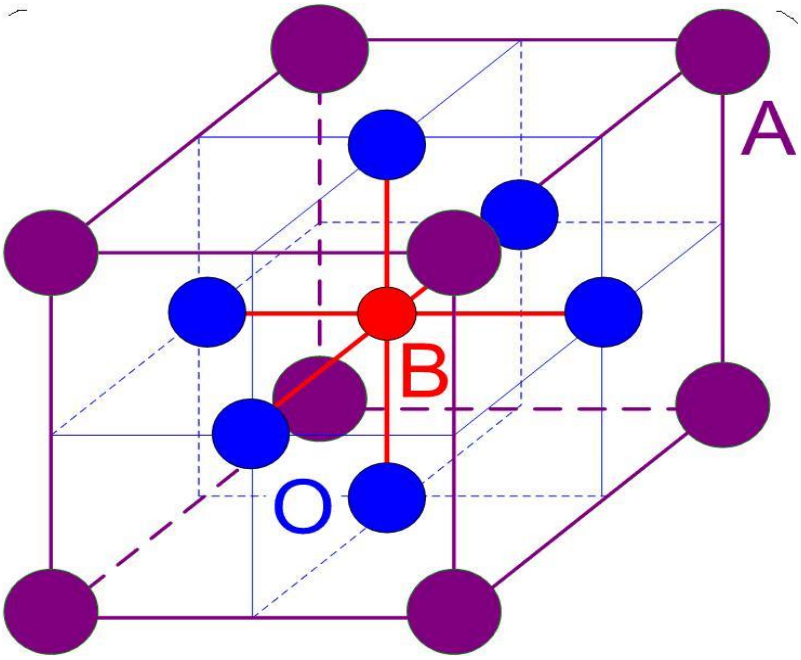

Fig. 4. ABO_3 perovskite structure

1.3. $Na_{0.5}Bi_{0.5}TiO_3$ and Related Materials

Most studied ferroelectric ceramics oxides with the perovskite structure due to their excellent physical properties (i.e., high dielectric constant, piezoelectric properties, ferroelectric

properties) include lead titanate ($PbTiO_3$), lead zirconate titanate ($Pb(Zr_xTi_{1-x})O_3$ or PZT), lead lanthanum zirconate titanate ($Pb_{1-x}La_x(Zr_yT_{1-y})_{1-x/4}O_3$ or PLZT), and lead magnesium niobate-lead titanate ($Pb(Mg_{1/3}Nb_{2/3}O_3)$- $PbTiO_3$, or PMN-PT) [6]. Despite their excellent ferroelectric & piezoelectric properties these materials contain a large amount of lead (> 60 wt. %) which is toxic. Therefore there is growing interest in developing lead free ferroelectric ceramics to replace lead based ferroelectric due to toxicity and concern for environmental protection [7]. Among various lead free perovskite systems, ($Na_{1/2}$ $Bi_{1/2}$) TiO_3 (NBT) is expected to be the candidate for lead free piezoelectric materials. $Na_{0.5}Bi_{0.5}TiO_3$ (NBT) is a complex perovskite ferroelectric ceramics, which was discovered by Smolenskii *et al* [8]. NBT is strongly ferroelectric at room temperature and undergoes diffuse phase transition with Curie temperature, $T_c=320^0C$. The remenant polarization $P_r=38$ $\mu C/cm^2$ and coercive field $E_c=73kV/cm$ at room temperature. It has also been reported from the structural and dielectric study that it displays two phase transformations, those are the cubic-to-tetragonal (515–525°C) and tetragonal-to-rhombohedral phase (255–265°C) transitions [9, 10]. The cubic–tetragonal transition corresponds to an electric order transformation from a paraelectric to an antiferroelectric (AFE) state, whereas the tetragonal–rhombohedral transition corresponds to a transformation from an antiferroelectric to a ferroelectric (FE) state [9]. However, this ceramic has drawbacks such as high conductivity and large coercive field (i.e., 73kV/cm), which cause problems during poling. This compound also posses low piezoelectric and electromechanical properties i.e. d_{33} of 92 pC/N and K_p coupling coefficients 18.6 [9, 11].

Among the various methodologies available in literature, one of the important methods to solve the above mention problems is suitable substitutions. In the present study, we have planned to substitute Nd at the A-site of the complex perovskite NBT.

1.4. Polymer Composite:

Now a days ferroelectric polymer composite also received considerable attention as compared to ferroelectric ceramics in view of their technological importance in devices such as sensors, actuators, transducers etc [12, 13]. Fabrication of composite materials means to combine two or more different materials having different properties to obtain the desirable material properties that often cannot be obtained in single-phase materials. Ceramics are less expensive and easier to synthesize than polymers or single crystals. Ceramics also have relatively high dielectric constants as compared to polymers and good electromechanical coupling coefficients. On the other hand, ceramics are disadvantageous due to their high acoustic impedance, which results in poor acoustic matching with media such as water and human tissue, which is the barrier for possible device applications. In addition, ceramics exhibit high stiffness and brittleness, which contributes to limited design flexibility. Ferroelectric polymer such as PVDF exhibits piezoelectric and pyroelectric response, low acoustic impedance which matches water and human skin and more over their properties can be tailored as per the requirement of the device. The best compromise in properties can be obtained by the judicious combination of piezoelectric ceramics and polymers. Piezoelectric ceramic/polymer composites possess high electromechanical coupling, low acoustic impedance, and an intermediate dielectric constant. Moreover, composites are flexible, and are moderately priced.

1.5. Materials under present investigation:

Based on the literature survey the materials under investigation are

$(Na_{0.5}Bi_{0..5})_{1-x}\,Nd_x\,Ti_{(1-x/4)}\,O_3$, x=0, 0.02, 0.04, 0.06

$Na_{0.5}Bi_{0.5}TiO_3$ (NBT)- PVDF composites

1.6. Objectives:

In view of the above importance of the ferroelectric polymer composites, the objectives are as follows:

- ✓ Synthesis of NBT and Nd- doped ceramics using solid state reaction techniques
- ✓ Structural characterization of powders by X-ray diffraction technique.
- ✓ Vibrational characterization using FTIR techniques.
- ✓ Microstructural characterization using Scanning Electron Microscopy (SEM)
- ✓ Synthesis of PVDF-NBT composite
- ✓ Characterization of the prepared composite by XRD and SEM

CHAPTER-2

SAMPLE SYNTHESIS

2.1. Introduction

The starting point of the materials science research is the synthesis of the desired materials. The synthesis of ceramic powders is important due to the increase in the requirements of ceramic materials for various industrial applications. Ceramic processing is a sequence of operations that systematically changes the chemical and physical aspects of the structure which ultimately affect the physical properties of the material. The aim of the science behind ceramic processing is to identify the important properties and to understand the effect of processing parameters on the structural and physical properties of the materials.

2.2. General Methods for Preparing Ceramic powders:

There are several techniques available in the literature for the synthesis of ceramic samples. There are mainly two approaches for synthesis. One is the chemical method and the other is the mechanical method. Mechanical methods are mainly of two type (a) Mixed oxide process or solid state reaction process and (b) High energy ball milling. Similarly, for the synthesis of the ceramics powder commonly used chemical methods are (a) Sol-gel methods, (b) Co-precipitation method, (iii) Hydrothermal Method (iv) Combustion Method etc. Both the chemical and mechanical methods have their own advantages and disadvantages. The mechanical method is successful for a large-scale production of bulk ceramic powders at its low cost and easy adaptability. In conventional solid-state method, high temperature and heating for prolonged time makes the particles coarse. Fine powders mainly prepared by chemical process have an improved homogeneity, densifications and the chemical precursors used in this process can easily be refined to increase the purity. However, in many cases, the chemical routes generally involve complex techniques when compared to the conventional solid state methods [14].

In the present study $Na_{0.5}Bi_{0.5}TiO_3$ and Nd modified $Na_{0.5}Bi_{0.5}TiO_3$ ceramics were prepared by the most economical mixed oxide process i.e., high temperature solid state reaction techniques.

2.3. Mixed Oxide Process:

This is a conventional method in which mostly oxides and carbonates are used as precursors. The processing of the material consists of the following steps. The raw materials (i.e., carbonates and oxides) are first weighed according to the stoichiometric formula of the desired ferroelectric ceramic. The raw materials are then thoroughly mixed (both dry and wet mixing) in an agate mortar for homogeneity. The mixture so obtained will be then put in a furnace to allow calcination in air atmosphere in an optimized condition. Calcination process is an endothermic decomposition reaction in which an oxy-salt, such as carbonate or hydroxide, decomposes leaving an oxide as a solid product and also liberating the gaseous products. The calcining temperature is important as it influences the density and hence the physical properties of the final product. Usually, the temperature of calcination is chosen high enough to complete the reaction to form the material, but the high temperature calcination may affect volatile oxides. So, the calcination temperature should be optimized for both the completion of reaction as well as prevention of volatile oxides. Double calcinations/recalcinations step is useful to get a homogeneous and single phase compound. The calcined powders will be cold pressed into cylindrical pellets by a hydraulic press with polyvinyl alcohol (PVA) as the binder. The use of the binder solution is to reduce brittleness of the pellets. The cold pressed specimens will then be sintered at higher temperature to achieve high density. Sintering is the process in which fine grains/powders are transferred to dense polycrystalline products after heating to an appropriate temperature below the melting point of the materials. Sintering is accompanied by the elimination of intergranular voids (pores) and by shrinkage of the whole system.

A flow chart of the Mixed Oxide method is given in Fig. 1.

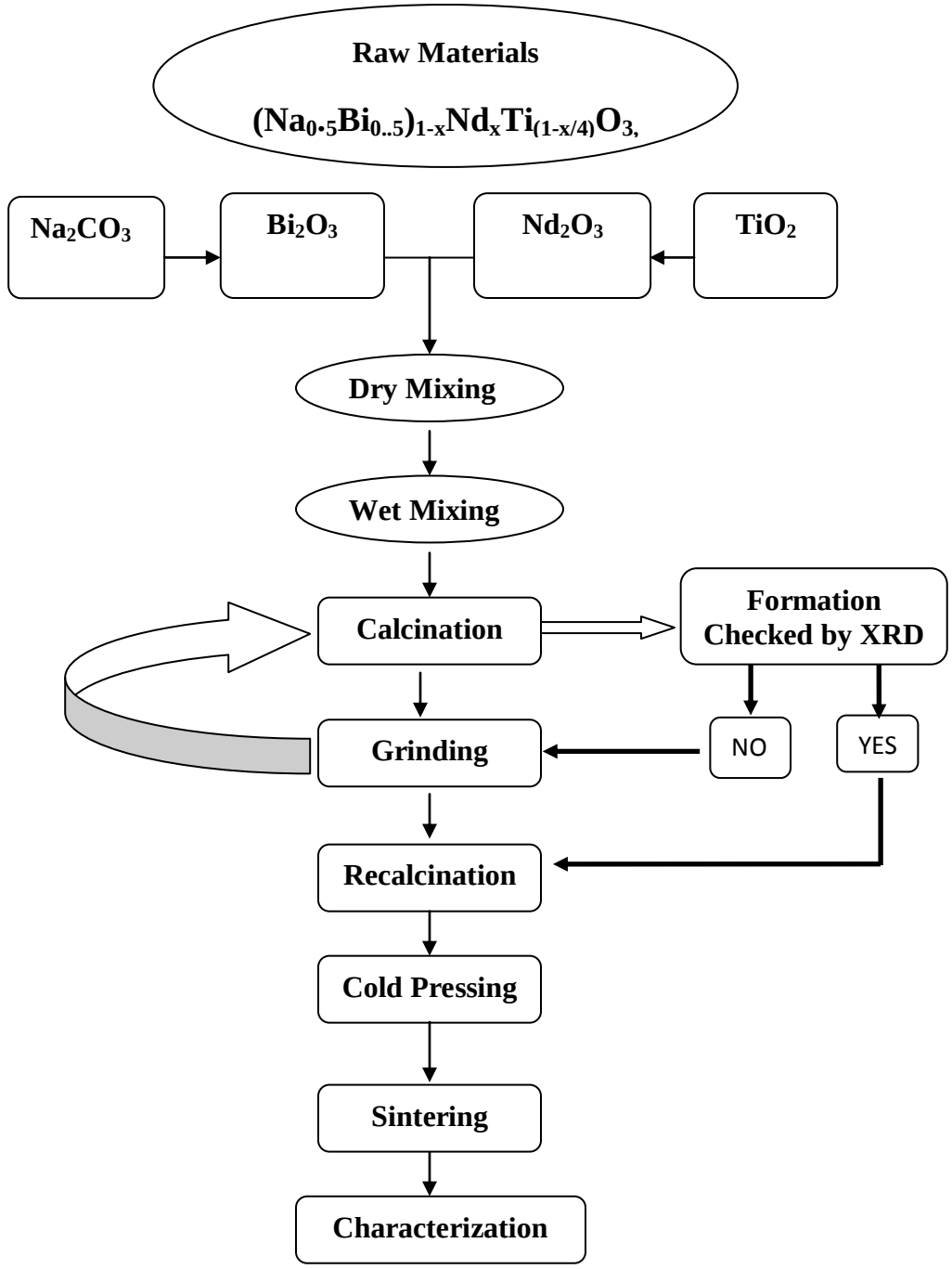

Fig. 1. Flow chart for the preparation of ceramics samples by a solid-state reaction technique.

The polycrystalline samples of $(Na_{0.5}\ Bi_{0.5})_{1-x}Nd_x\ Ti_{(1-x/4)}O_3$ with x=0.0, 0.02, 0.04, and 0.06 were prepared from the following carbonates and oxides: Sodium carbonates (Na_2CO_3), Bismuth Oxides ($Bi_2O_{3)}$, Titanium Oxide (TiO_2) and Neodymium Oxide (Nd_2O_3). A conventional solid state reaction technique has been adopted to prepare the materials. The ingredients were thoroughly mixed and ground in dry condition for 3h, and in acetone for 1h in an agate mortar to get homogenous mixture of the materials. Then the mixed powders of the compounds were calcined at 950^0C in an alumina crucible for 4 h in an air atmosphere. Then the powders were grinded again and calcination was repeated at 1050^0C for 4 h in an air atmosphere. The quality and formation of the compounds were checked by an X-ray diffraction (XRD) technique. The fine and homogeneous powder of the above compounds were pressed into cylindrical pellets of 10 mm diameter and 1-2 mm thickness under a uniaxial pressure of $6x10^6$ N/m^2 using a hydraulic press. Polyvinyl alcohol (PVA) was used as a binder to reduce the brittleness of the pellets. The pellets were then sintered for 4 h at 1100^0C in air atmosphere. The binder was burnt out during the high temperature sintering. The formations of the prepared compounds were studied by an X-ray diffraction technique (XRD).

2.4. Preparation of NBT-PVDF Composites:

After the preparation of NBT ceramic powder, the composite is prepared using cold pressing technique as shown in the flow chart given in Fig. 2. About 1gm of the polyvinlydene fluoride (PVDF) polymer was dissolved in 10 ml of ethyl methyl ketone and the solutions were then stirred vigorously for 24h to facilitate proper mixing. Then 10 wt % (i.e., 0.1 gm) of $Na_{0.5}Bi_{0.5}TiO_3$ ceramic powder was added into it and the whole contents were again stirred for 24

hours. Then it was allowed to dry at room temperature. Then it was grinded and cold-pressed to get the desired size of the composite pellet.

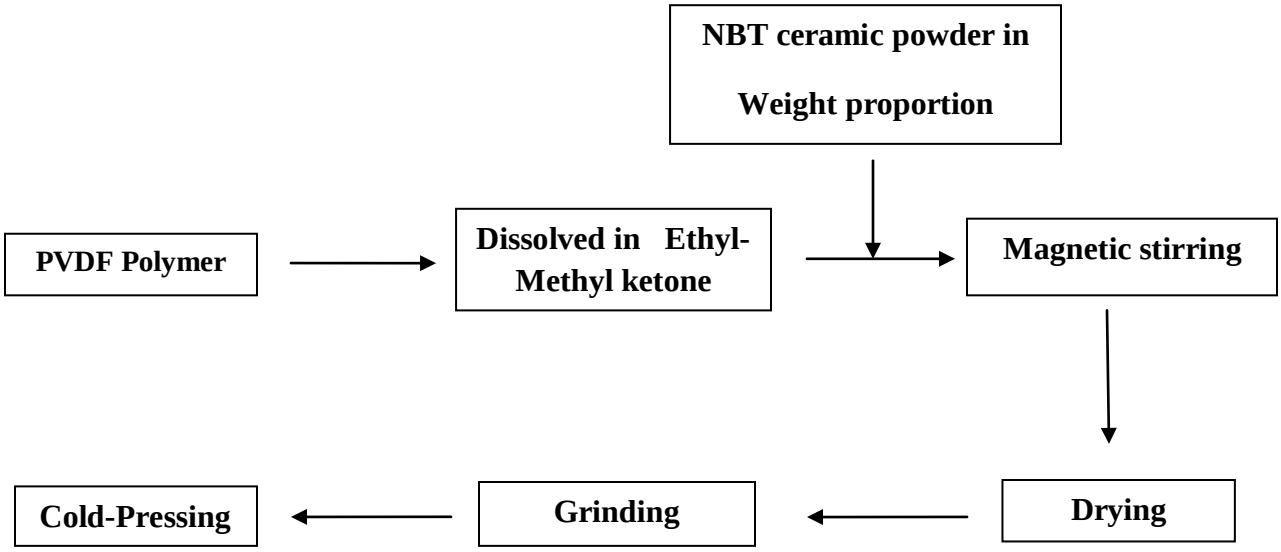

Fig. 2 Flow chart for the preparation of NBT-PVDF Composites

2. 5. Characterization:

The X-ray diffraction technique is used to determine the atomic arrangements (i. e., crystal structure) of the materials because the interplanar spacing (d-spacing) of the diffracting planes is of the order of X-ray wavelength. For a crystal of given d-spacing and wavelength λ, the various orders n of reflection occurs only at the precise values of angle θ which satisfies the Bragg condition

$$2d \sin\theta = n\lambda$$

The accurate determination of interplanar spacing, lattice parameters etc. provides an important basis in understanding of various physical properties of materials.

For structural characterization of the material, he X-ray diffraction (XRD) patterns of all the compounds have been recorded at room temperature (25^0C) using X-ray powder diffractometer (Philips X-ray diffractometer) with Cuk_α radiation (λ = 1.5405 Å) in a wide 2θ (Bragg angle) range ($20^0 \leq 2\theta \leq 80^0$) at a scanning rate of 3^0/min. Fourier transform infrared (FTIR) spectra of the of the present studied ceramics oxides were recorded with a FTIR spectrometer (Model: Perkin Elmer) from 4000 to 400 cm^{-1} with a resolution of 2 cm^{-1}.

The scanning electron microscopy (SEM) is a versatile tool to characterize microstructures of the samples. SEM makes use of point to point scanning of the solid surface and produces a clear image of specimens, which can be visible with a naked eye and provides information about their size which lies in the range of μm. The surface morphology/microstructural studies of the material sample have been carried out using a computer-controlled scanning electron microscope (SEM) (JEOL T-330). The sample pellets were platinum coated prior to being scanned under high-resolution field emission gun scanning electron microscope.

CHAPTER-3

RESULTS AND DISCUSSION

The room temperature x-ray diffraction patterns of Nd –modified NBT (i.e. $(Na_{0.5}Bi_{0..5})_{1-x}Nd_xTi_{(1-x/4)}O_3$, x=0, 0.02, 0.04, 0.06) are shown in Figure-1.

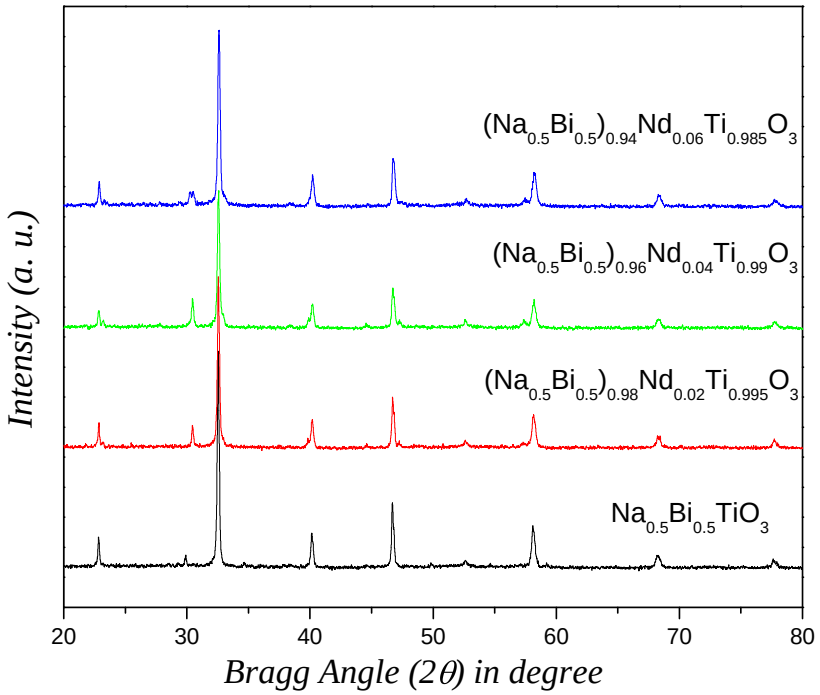

Fig. 1 x-ray diffraction patterns of Nd-modified NBT

The sharp and well defined single diffraction peaks, which were different from those of the ingredients confirms the formation of the compound in perovskite structure. Both in XRD patterns of NBT and Nd-modified NBT, a small percentage of pyrochlore phase is observed (around the peak position of 27^0) along with the desired compounds. The intensity of the pyrochlore phase increases with increase in Nd substitution at A site of NBT. It has also been observed that, there is a change in the peak position, peak intensity & peak shape of NBT on increasing Nd content. Using 2θ values, interplaner spacing (d) of each peak was calculated using the Bragg's law of diffraction. All the XRD peaks of all the compounds were indexed in

different crystal systems and unit cell configurations using a computer program POWDMULT [15]. The best agreement in observed and calculated 2ɵ (i.e., $\Delta\theta$ ($2\theta_{obs}$-$2\theta_{cal}$) = minimum) and d values ($\sum\Delta d$= (d_{obs}-d_{cal}) = minimum) were found for rhombohedral for x= 0.0 and 0.02, tetragonal for x=0.04 and cubic for x=0.06 respectively. The crystal system, unit cell parameters, comparison of observed and calculated d-values, miller indices and the relative intensity for different compositions of $(Na_{0.5}Bi_{0..5})_{1-x}Nd_xTi_{(1-x/4)}O_3$ are shown in the Tables 1-4.

Table-1: sample:$Na_{0.5}Bi_{0.5}TiO_3$ **Crystal Structure**: Rhombohedral

a = 5.4933A^0 b=5.4933A^0 c=13.5048 A^0

$\alpha=90^0$ $\beta=90^0$ $\gamma=120^0$

Sl. No.	d-spacing		I/I_0	Miller Indices		
	d-observed A^0	d-calculated A^0		h	k	l
1	3.8936	3.8891	13.31	1	0	2
2	2.7497	2.7467	100	1	1	0
3	2.2438	2.2435	14.04	2	0	2
4	1.9428	1.9445	58.15	2	0	4
5	1.7381	1.7376	1.97	1	1	2
6	1.5858	1.5858	18.50	3	0	0
7	1.3730	1.3733	5.56	2	2	0
8	1.2278	1.2277	2.87	0	1	1

Table: 2 Sample: $(Na_{0.5}Bi_{0.5})_{0.98}Nd_{0.02}Ti_{0.995}O_3$ **Crystal Structure**: Rhombohedral

a=5.4917A^0 b=5.4917A^0 c=13.5048A^0

$\alpha=90^0$ $\beta=90^0$ $\gamma=120^0$

Sl. No.	d-spacing		I/I0	Miller Indices		
	d-observed A^0	d-calculated A^0		h	k	l
1	3.8920	3.8883	13.53	1	0	2
2	2.7484	2.7459	100	1	1	0
3	2.2426	2.2430	15.53	2	0	2
4	1.9423	1.9442	28.86	2	0	4
5	1.7372	1.7371	2.29	2	1	2
6	1.5848	1.5853	19.54	3	0	0
7	1.3733	1.3729	3.30	2	2	0
8	1.2278	1.2277	5.14	0	1	1

Table-3: Sample: $(Na_{0.5}Bi_{0.5})_{0.96}Nd_{0.04}Ti_{0.99}O_3$ **Crystal Structure**: Tetragonal

a=5.4875A^0 b=5.4875A^0 c=3.8889A^0

$\alpha = 90^0$ $\beta = 90^0$ $\gamma = 90^0$

Sl. No.	d-spacing		I/I0	Miller Indices		
	d-observed A^0	d-calculated A^0		h	k	l
1	3.8909	3.8889	13.15	0	0	1
2	2.7478	2.7468	100	1	1	1
3	2.2415	2.2419	14.89	2	0	1
4	1.9385	1.9401	15.69	2	2	0
5	1.7382	1.7384	3.57	1	1	2
6	1.5844	1.5847	18.9	3	1	1
7	1.3724	1.3719	6.82	4	0	0
8	1.2274	1.2273	3.58	3	3	1

Table-4 Sample: $(Na_{0.5}Bi_{0.5})_{0.94}Nd_{0.06}Ti_{0.985}O_3$ **Crystal Structure**: Cubic

a=3.8810A^0 b=3.8810A^0 c=3.8810A^0

$\alpha=90^0$ $\beta=90^0$ $\gamma=90^0$

Sl. No.	d-spacing		I/I0	Miller Indices		
	d-observed A^0	d-calculated A^0		h	k	l
1	3.8852	3.8810	13.67	1	0	0
2	2.7452	2.7443	100	1	1	0
3	2.2413	2.2407	14.18	1	1	1
4	1.9406	1.9405	26.69	2	0	0
5	1.7363	1.7356	2.59	2	1	0
6	1.5835	1.5844	17.08	2	1	1
7	1.3725	1.3721	2.56	2	2	0
8	1.2270	1.2273	3.12	3	1	0

This indexing of XRD patterns with the above crystal systems are in agreement with the reported one for La doped NBT [9].

The broadening of x-ray diffraction peaks are mainly due to the small crystallite size and strain. To separate the contribution of crystallite size and r.m.s. strain, we have plotted the Willamson-Hall plot using the following equation [16, 17]:

$$\frac{\beta\cos\theta}{\lambda} = \frac{1}{D} + \frac{4\varepsilon\sin\theta}{\lambda}$$

Where β=is the FWHM (full width at half maxima) of the profile in radian, θ= Bragg diffraction angle, λ= incident wave length, D= crystallite size and ε= r. m. s. strain. By plotting βcos θ/ λ vs. sinθ/ λ, r. m. s. strain can be calculated from the slope and the crystallite size can calculated from the ordinate intercept.

Figures 2-5 shows the Willamson-Hall of $(Na_{0.5}Bi_{0..5})_{1-x}Nd_xTi_{(1-x/4)}O_3$ with different values of x.

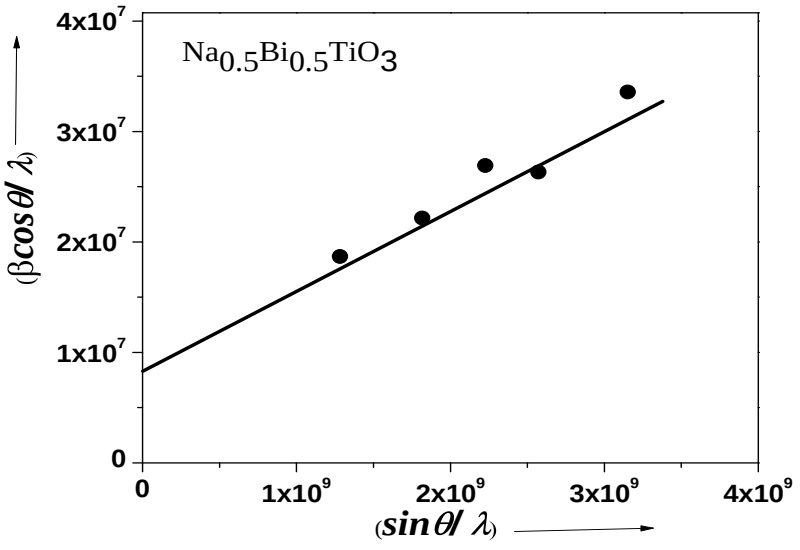

Fig. 2 Willamson-Hall plot of $(Na_{0.5}Bi_{0..5})$ TiO3

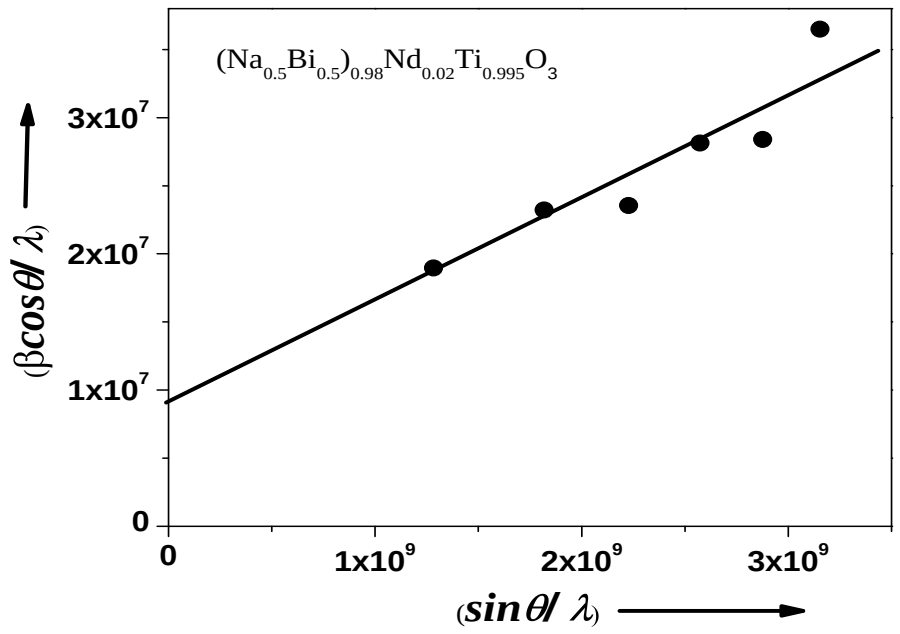

Fig. 3 Willamson-Hall plot of $(Na_{0.5}Bi_{0.5})_{0.98}Nd_{0.02}Ti_{0.995}O_3$

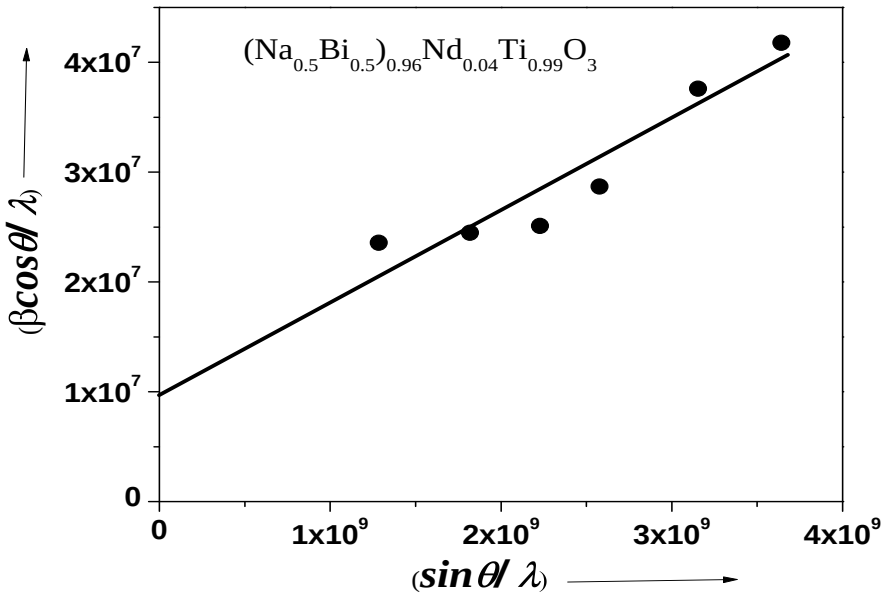

Fig. 4 Willamson-Hall of $(Na_{0.5}Bi_{0.5})_{0.96}Nd_{0.04}Ti_{0.99}O_3$

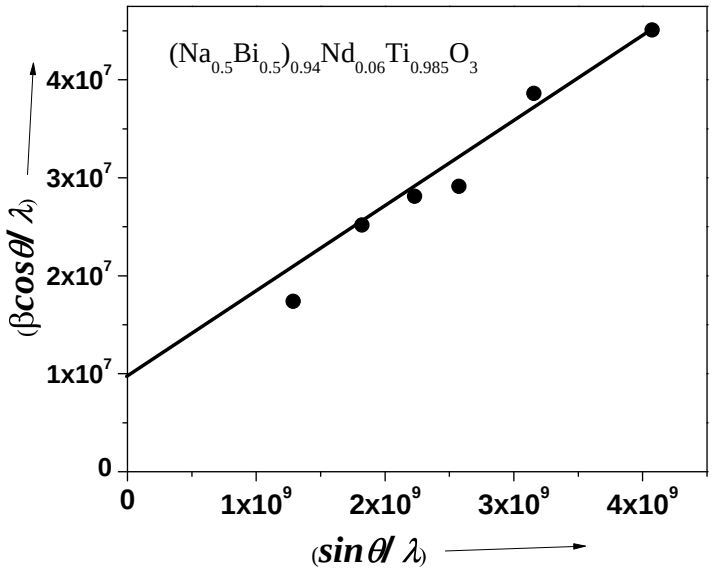

Fig. 5 Willamson-Hall of $(Na_{0.5}Bi_{0.5})_{0.96}Nd_{0.04}Ti_{0.985}O_3$

The calculated value of crystallite size and r. m. s. strain is compared in Table 5.

Table 5

Sample name	*Size in nm*	*rms strain* $\times 10^{-3}$
$(Na_{0.5}Bi_{0..5})$ TiO3	*118*	*1.79*
$(Na_{0.5}Bi_{0.5})_{0.98}Nd_{0.02}Ti_{0.995}O_3$	*108*	*1.86*
$(Na_{0.5}Bi_{0.5})_{0.96}Nd_{0.04}Ti_{0.99}O_3$	*103*	*2.06*
$(Na_{0.5}Bi_{0.5})_{0.96}Nd_{0.04}Ti_{0.985}O_3$	*101*	*2.15*

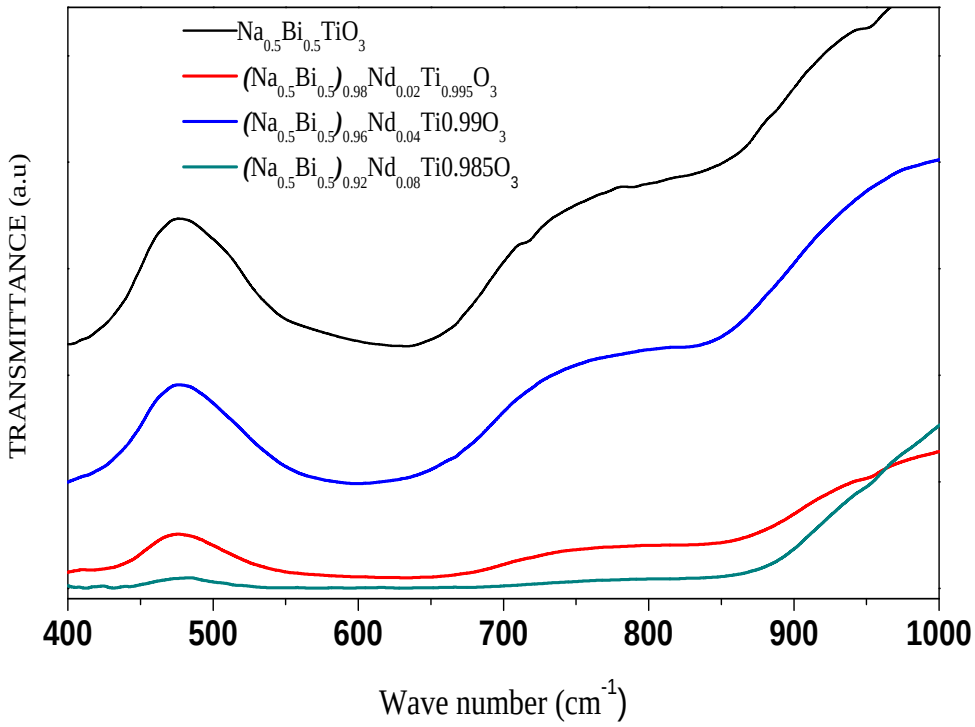

Fig-6 Room temperature FTIR spectra of $(Na_{0.5}Bi_{0..5})_{1-x}Nd_xTi_{(1-x/4)}O_3$, (x=0, 0.02, 0.04, 0.06)

The room temperature FTIR spectra of $(Na_{0.5}Bi_{0..5})_{1-x}Nd_xTi_{(1-x/4)}O_3$ for different value of x (i.e., x=0, 0.02, 0.04, 0.06) in the region 400-1000 cm^{-1} is shown in Fig. 6. The FTIR pattern is characterize by the appearance of a broad peak around 600 cm^{-1} and one shoulder around 850 cm^{-1}. The bands in the low-wave number region are assigned to Ti–O bond vibrations [18]. For all the studied samples, the observed band around 600 cm^{-1} represents the characteristics vibarations of Ti-O octahedral and indicates the formation of the perovskite phase. There is a change in the peak position, peak intensity and width of the characteristic peak on addition of Nd.

Fig.7 show the SEM micrographs of the $(Na_{0.5}Bi_{0..5})_{1-x}Nd_xTi_{(1-x/4)}O_3$ for x=0.0, 0.02.

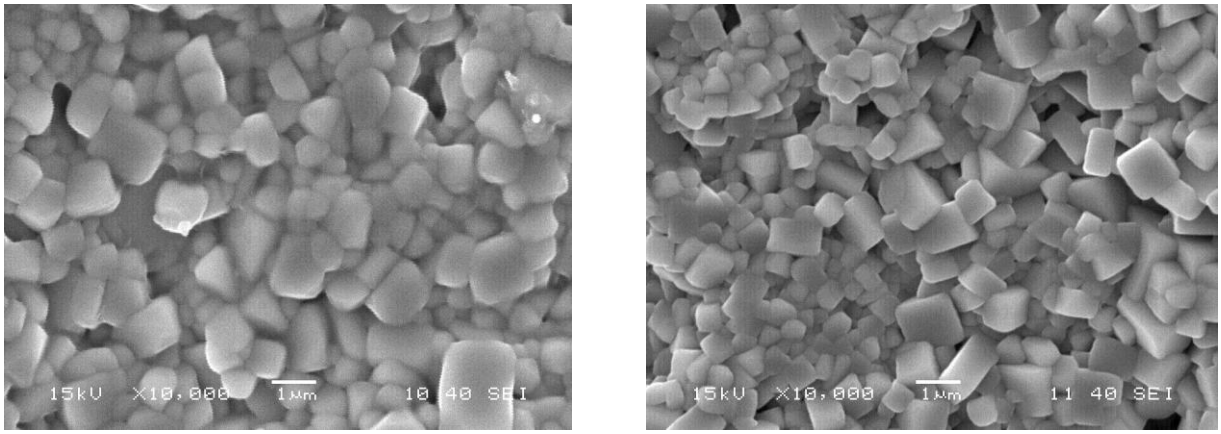

(a) **(b)**

Fig. 7 SEM micrographs of $(Na_{0.5}Bi_{0..5})_{1-x}Nd_xTi_{(1-x/4)}O_3$ (i.e., (a) x=0.0 and (b) x= 0.02)

The SEM micrographs indicate the existence of polycrystalline microstructure of the ceramic oxide sample comprising of rectangular or square shape grains with shape anisotropy. It has been evident that grains are well defined and uniformly distributed with certain degree of agglomeration and porosity. The average grain size are found to be nearly 1 & 0.5 micrometer for x=0, 0.02 respectively. So on addition of Nd there may be decrease in the grain size of the samples.

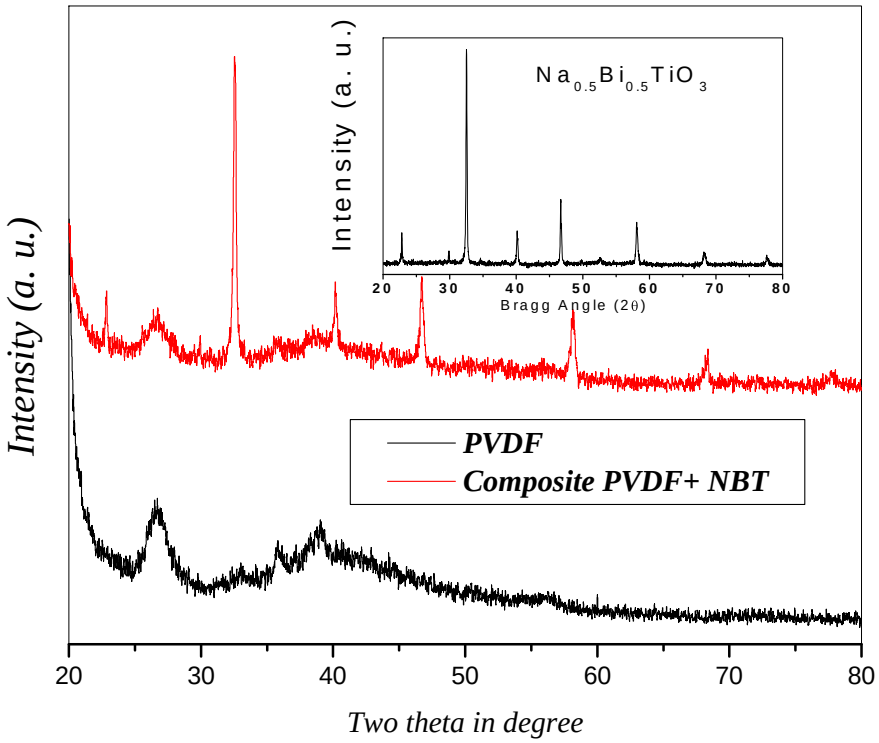

Fig. 8 X-ray diffraction pattern of PVDF, NBT and the composite.

Fig. 8 shows the x-ray diffraction pattern of PVDF, NBT and the composite. The XRD pateern of PVDF has a typical feature of background hump followed by several broadened characteristic diffraction peaks. This feature indicates that the polymer (i.e., PVDF) are composed of a combination of crystalline and amorphous phases. From the XRD pattern of the composite, it has been observed that all the peaks are coming from the contributions either from the ceramics oxides or from the polymer host itself. This result suggests that the ceramic oxides are embedded in the polymer matrix. In order find out how the distribution of ceramic oxides in the polymer matrix we have carried out the energy dispersive x-ray dot mapping analysis and SEM analysis.

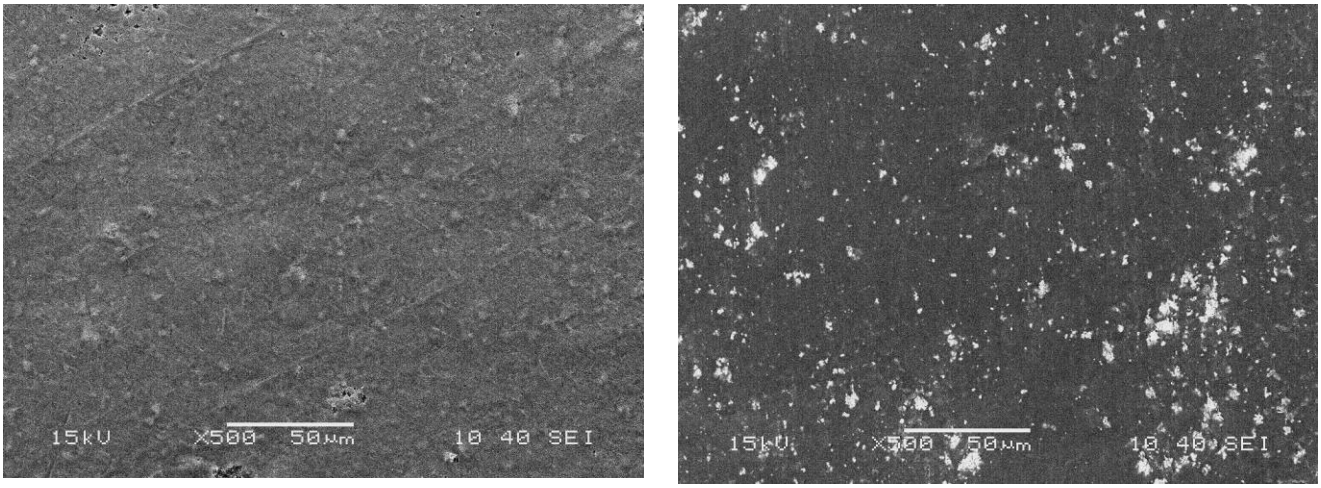

(a) **(b)**

Fig. 9 SEM micrographs of (a) PVDF and (b) NBT-PVDF composite

Fig. 9 shows the SEM micrographs of PVDF and NBT-PVDF composite. In case of the micrographs of polymer, only smooth suface is observed. However in case of the composite the ferroelectric ceramic oxides are distributed on the polymer matrix. In SEM micrographs of the composites, the light area corresponds to the ferroelectric ceramics and the drak region corresponds to the polymer matrix.

Energy dispersive X-ray (EDX) analysis was carried out in order to find out the distribution of a particular element (in the present study ferroelectric ceramics oxides) in polymer composite. X-ray mapping generates a two-dimensional image to get even better ideas of the relative distribution of elements. Maps for multiple elements can also be collected so that we can get an idea of the elemental distribution of the materials.

(Dot mapping of Bi in Composite) (Dot mapping of Ti in Composite)

Fig. 10 Dot map of the distribution of Bi and Ti element as representative of ceramics in NBT-PVDF composites

Fig.10 represents the x-ray dot maps of Bi and Ti element in the polymer composite. The uniformity of the white dots (representative of Bi and Ti), indicates that the NBT are homogenously dispersed in the polymer. No aggregation of the filler particles is evident in Fig. 10.

CONCLUSIONS

In the present work, we have prepared and studied the complex perovskite ceramics oxides having the general chemical formula $(Na_{0.5}Bi_{0..5})_{1-x}Nd_xTi_{(1-x/4)}O_3$, and the composite of PVDF and NBT. The structural (XRD), microstructural/morphological and vibrational properties of the proposed compounds have been extensively studied.

Based on our results following conclusions have been drawn.

- NBT and Nd-modified NBT were prepared by high temperature solid-state route and the polymer ceramic composite was prepared by cold press technique.
- The formation of the ceramic in perovskite structures and polymer composite were confirmed by XRD analysis.
- The lattice parameters are calculated by using standard software POWD.
- Williamson Hall method is used for finding the crystallite size and strain in the samples.
- Microstructures/morphology of the materials were analyzed by scanning electron microscopy.
- Studies of FTIR spectroscopy confirm formation of perovskite structure of the ferroelectric ceramics.

REFERENCES

[1] G. H. Haertling, J. Am. Ceram. Soc., 82[4], (1999) 797.

[2] A. Safri, R. K. Panda, Victor F. Janas, "Ferroelectric Ceramics: Processing, Properties & Applications". Rutgers University, Piscataway NJ 08855, USA.

[3] Kenji Uchino, "Ferroelectric Devices", Marcel Dekker Inc, New York, 2000.

[4] Charles Kittel, Introduction to Solid State Physics, Wiley India Edition, 2008

[5] J. Valasek, Phys. Rev., 15, (1920) 537- 538.

[6] T. Takenaka, K. Maruyama, K. Sakata, Japan. J. Appl. Phys. 30 (1991) 2236.

[7] T. Takanaka, H. Nagata, J. Euro. Ceram. Soc. 25 (2005) 2693.

[8] V. A. Isupov, *Ferroelectrics*, 315 (2005) 123.

[9] A. Herabut and A. Safari, J. Am. Ceram. Soc., 80 (1997) 2954.

[10] G. O. Jones, P. A. Thomas, Acta Crystallography. B, 58 [2], (2002) 168

[11] C. F. Buhrer, J. Chem. Phys., 36, (1962) 798.

[12] A Safari, J . Phys. III. France 4(1994) 1129.

[13] R. E. Newnham, L. J. Bowen, K. A. Klicker, L. E. Cross, Materials in engineering, 2 (1980) 93.

[14] W. C. Lee, C. Y. Huang, L. K. Tsao, Y. C. Wu, J. Euro. Ceram. Soc., 29 (2009) 1443.

[15] "POWD" an interactive powder diffraction data interpretation and indexing programme Vs. 2.1, E. Wu, School of Physical Sciences, Flinder University of South Australia, Bedford Park, SA-5402, Australia

[16] Sanjay K. Rai, Anish Kumar, Vani Shankar, T. Jayakumar K. Bhanu Sankara Rao, Baldev Raj Scripta Materialia 51 (2004) 59–63

[17] K. Kapoor, D. Lahiri, S. V. R. Rao, T. Sanyal and B. P. Kashyap, Bull. Mater. Sci. 27 (2004) 59

[18] J. T. Last, Phys. Rev., 105 (6) (1957) 1740.